Supporting Information

Experimental Section

Polyoxometalate synthesis

$TBA_4(SiW_{12}O_{40})$ was synthesised according to Rocchiccioli-Deltcheff.[1] The process involved cation exchange by addition of an aqueous saturated solution of tetrabutylammonium bromide (Sigma-Aldrich, 99.0%) to an aqueous saturated solution of tungstosilicic acid hydrate (Sigma-Aldrich, 99.9%). This produced precipitation of $TBA_4(SiW_{12}O_{40})$, which was filtered, and then recrystallized using a 1:1 mixture of acetonitrile (Sigma-Aldrich, 99.8 %) and diethyl ether (Sigma-Aldrich, 98.0%). $TBA_4(SiW_{12}O_{40})$ was dried under vacuum (<1 mbar) at 120 ^oC for 48 hours and then stored in a dry argon-filled glovebox (< 10 ppm O_2, < 10 ppm H_2O, MBRAUN).

Electrolyte preparation

Dimethyl sulfoxide (anhydrous, Sigma-Aldrich, 99%), was dried using dry 4 Å molecular sieves (beads, 4-8 mesh, Sigma-Aldrich). As received molecular sieves were dried by heating under vacuum (< 1 mbar) at 250 ^oC for 48 hours. The water content of the dried solvents was found to be between 10-15 ppm by using a Karl-Fischer titration (Metrohm 831 KF coulometer).

Lithium bis(trifluoromethylsulfonyl)imide (LiTFSI, Sigma-Aldrich, 99.95%), was dried under vacuum (< 1 mbar) for 48 hours at 120 °C.

After drying, all solvents and reagents were stored in a dry argon-filled glovebox (< 10 ppm O_2, < 10 ppm H_2O, MBRAUN) until use. Solutions were prepared inside the glovebox by dissolving the appropriate amounts of salt and redox mediator in the chosen solvent. Solutions were left to stir on a magnetic stirrer in the glovebox until fully dissolved. Solutions were used on the same day as they were prepared.

Cyclic voltammetry experiments in a two-compartment glass cell

All electrochemical measurements were performed using a Bio-Logic variable multichannel potentiostat (VMP2).

Cyclic voltammetry measurements were performed using a two-compartment glass U-cell, containing a porous glass frit that allowed the separation of the working electrode compartment and the reference electrode compartment. In this way, the measurements are not affected by the reaction of the mediator with the reference electrode, since in all cases, the solution in the reference electrode compartment contained no mediator. The U-cell assembly was carried out in a dry argon filled glovebox to ensure an inert atmosphere prior to cycling.

The working electrode consisted of a glassy carbon rod (Alfa-Aesar, 1.5 mm radius) encased in glass. The electrode was polished with 25 µm followed by 1 µm and then 0.3 µm aluminium oxide powder (Buehler) for 1, 2 and 5 minutes respectively.

$Li_{0.5}FePO_4$ affixed to a stainless steel mesh was used as counter and reference electrode. The $Li_{0.5}FePO_4$ reference electrodes was made with a composite prepared with 1.6 g of $LiFePO_4$ (Tatung), 1.6 g $FePO_4$, 0.4 g acetylene black (Chevron Phillips Chemical Company) and 2.6 g PTFE (DuPont). $FePO_4$ was prepared as described in[2]. The materials were mixed and grinded with a pestle and mortar for 10 minutes, after which a sheet of around 0.5 mm thickness was obtained using a rolling mill (Durston), and 25 mm diameter electrodes were punched and dried under vacuum (< 1 mbar) at 120 ^oC for 48 hours.

Galvanostatic cycling in Swagelok cells

Stainless steel 1" Swagelok-style cells were used with a home-made stainless steel plunger that allowed the cells to be purged with oxygen. The inside of the stainless steel cell was electronically insulated from the cell stack using an insulating sheet of fluorinated ethylene propylene, FEP (0.127 mm thick). PTFE ferrules from Swagelok were employed. A piece of lithium ion conducting glass ceramic (LICGC™, Ohara Corporation, Ø = 1 inch) was incorporated within the cell to separate the working and reference electrode compartments, to ensure the reaction of redox mediators at the reference electrode was avoided. Ohara has good conductivity of lithium ions and blocks the transport of other species.

The cells contained the following: a $Li_{0.5}FePO_4$ counter electrode (Ø = 25 mm), a Celgard® 3401 separator (Ø = 25 mm) wetted with 50 µl of the electrolyte without redox mediator, a lithium ion conducting glass ceramic (LICGC™, Ohara Corporation, Ø = 1 inch), a Celgard® 3401 separator (Ø = 25 mm) wetted with 50 µl of the electrolyte without redox mediator, and a carbon cloth (Ø = 20 mm) (Freudenberg H23, Quintech) working electrode wetted with 50 µl of the electrolyte with redox mediator.

The bottom half of each Swagelok® cell was pre-assembled outside the glovebox and all components were dried under vacuum (<1 mbar) at 80 ^oC overnight. Then, the cell components were transferred to the glovebox, and were left to cool to the ambient temperature of the glove box before complete cell assembly was done.

The experiments in an argon atmosphere were done with the cells as assembled inside the argon-filled glovebox. For the experiments in an oxygen atmosphere, the cells were purged with oxygen (BOC, 99.999%) at a pressure of 1.1 atm for 30 seconds. Then, the cells were transferred to a temperature controlled oven at 25 ^oC for the electrochemical cycling, which was initiated 60 minutes post-transfer to ensure cell equilibration. Galvanostatic cycling was completed at currents equal to 50 µA, 100 µA and 200 µA which correspond to current densities (normalized by the geometrical area of the electrode) of 15.9 µA cm^{-2}, 31.8 µA cm^{-2} and 63.7 µA cm^{-2} respectively.

XRD characterization

XRD measurements were performed on a Rigaku SmartLab instrument with a copper X-ray source using grazing incidence. The 2-theta angle range was set to scan from 20 -70 degrees using a 0.2 degree 2-theta increment. A scan of 12 hours was performed overnight on the discharged cathode.

A Swagelok cell containing a carbon-coated Celgard cathode (Ø = 13 mm) with 50 mM $TBA_4SiW_{12}O_{40}$ in 1 M LiTFSI DMSO was purged with O_2 and subject to a current of 20 µA (corresponding to 15 µA cm^{-2}) up to 2.5 V vs. Li^+/Li for 96 hours. Immediately after discharge, the cell was transferred to an argon-filled glove box and the cathode was removed from the cell and transferred to a hemispherical air tight sample holder (Bruker, A100B33) for XRD measurements.

The carbon-coated Celgard cathode contained 66% wt. acetylene black and 33% wt. lithiated Nafion. Inks were made with 0.2 g acetylene black, 1 g of lithiated Nafion solution (Ion Power, 10% wt.) and 4 ml isopropyl alcohol. The above quantities were added to a glass vial and stirred for 3 hours, homogenised (IKA®) at 10,000 rpm for 5 minutes and then homogenised at 20,000 rpm for a further 5 minutes. The slurry was cast over Celgard® 3401 separator using a 200 µm K Hand Coater. Once dry, working electrodes (Ø = 13 mm) were punched out between paper sheets. The electrodes were dried under vacuum (<1 mbar) at room temperature for 48 hours. The carbon loading in the electrodes was ca. 0.35 mg cm^{-2}.

O_2 consumption analysis

The evaluation of the number of moles of oxygen consumed during discharge from in-situ pressure change measurements was carried out as follows. After the experiments, the internal volume of Swagelok cells were determined using an EL-CELL® pressure gauge with a known internal volume of 3 ml. The Swagelok cells were connected to the pressure gauge using Swagelok connections and PEEK tubing, with a Swagelok needle valve used to isolate each system. The pressure of gas in the pressure gauge was set to ca. 1.8 bar, while the pressure in the Swagelok cell was set to between 1- 1.8 bar. Upon opening the needle valve connecting the Swagelok cell to the pressure gauge, the pressure of the system equilibrated. The volume of the Swagelok cells was then determined using the following equation.

$$P_{cell}V_{cell} + P_G V_G = P_{tot}(V_{cell} + V_g)$$

where P_{cell} and P_G are the pressure values within the cell and the pressure gauge, respectively, before equilibration, P_{tot} is the total pressure in the system after opening the needle valve, and V_{cell} and V_G are the volumes of the cell and the pressure gauge, respectively.

Once the internal volume of the cell has been determined, it was possible to determine the number of moles of oxygen consumed during discharge from the change in pressure in the system using the Ideal Gas Law:

$$PV = nRT$$

where *P* is the pressure in the system (bar), *V* is the internal volume of the system (*L*), *n* is the number of moles (*mol*), *R* is the ideal gas constant (0.08314 *bar L* K^{-1} mol^{-1}) and *T* is the temperature in *K*.

For the experiments reported in figure 3 in the main article, the internal volumes of the Swagelok cells with and without $TBA_4SiW_{12}O_{40}$ were = 6.55 ml and 5.28 ml, respectively.

Additional figures and tables

Cyclic voltammetry measurements of a glassy carbon in a solution containing 10 mM $TBA_4SiW_{12}O_{40}$ were performed with a low potential limit of 1.9 V vs. Li^+/Li (figure S1). A two-compartment glass cell was used (as detailed above) with 10 mM $TBA_4SiW_{12}O_{40}$ in 1 M LiTFSI DMSO in the working compartment and 1 M LiTFSI DMSO in the reference compartment. Experiments were performed with argon saturated solutions, and the results show the multiple redox processes of $TBA_4SiW_{12}O_{40}$.

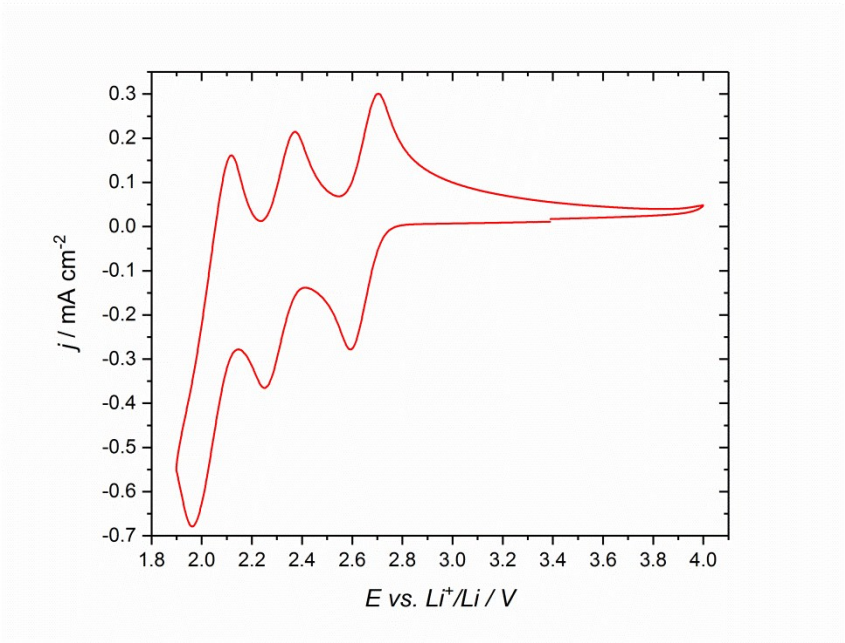

Figure S1: Cyclic voltammogram of a glassy carbon electrode in an argon-saturated solution with 10 mM $TBA_4SiW_{12}O_{40}$ in 1 M LiTFSI in DMSO Scan rate: 20 mV s^{-1}.

Additional cyclic voltammetry measurements were performed at different scan rates (figure S2). Values of peak potentials vs. peak currents were plotted in figure S3, from which an extrapolation to zero current provided a peak to peak separation of 68 mV. For these experiments, prior to cyclic voltammetry, impedance measurements were performed to obtain the uncompensated solution resistance (660 Ohms), and manual IR compensation with an 85% correction was applied during cyclic voltammetry measurements using the EC-lab software.

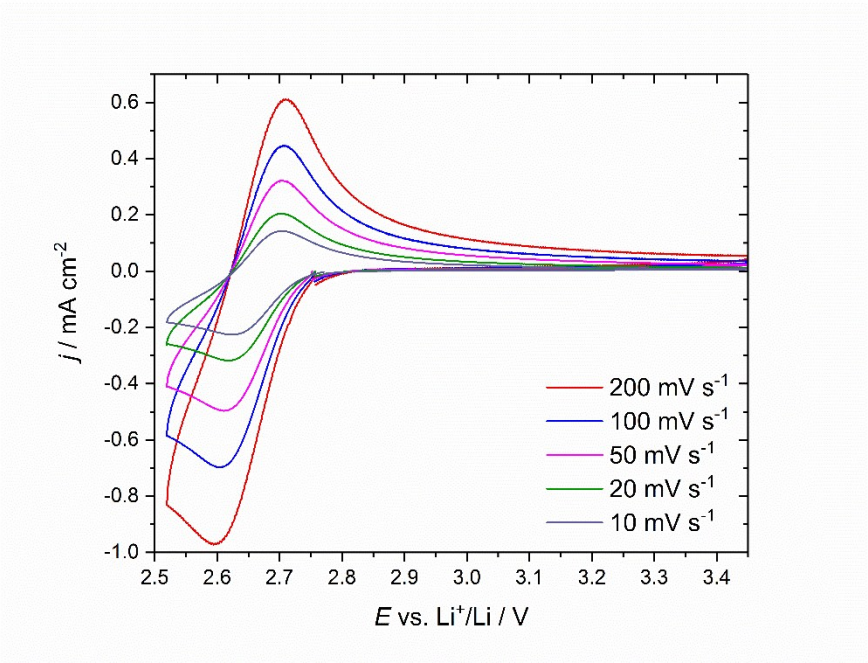

Figure S2: Cyclic voltammograms of a glassy carbon electrode in an argon-saturated solution with 10 mM $TBA_4SiW_{12}O_{40}$ in 1 M LiTFSI in DMSO, recorded at scan rates of 10, 20, 50, 100 and 200 mV s^{-1}, swept negative from the open circuit potential with manual IR compensation (85%)**.**

Table S1: Peak currents (I_{pc} and I_{pa}), peak potentials (E_{pc} and E_{pa}) and peak-to-peak separation (ΔE), as obtained from the results in figure S2

Scan Rate / mV s^{-1}	E_{pc} vs. Li^+/Li / V	I_{pc} / mA cm^{-2}	E_{pa} vs. Li^+/Li / V	I_{pa} /mA cm^{-2}	ΔE / mV
200	2.59	-0.98	2.71	0.62	115
100	2.61	-0.70	2.71	0.45	102
50	2.61	-0.50	2.70	0.32	93
20	2.62	-0.32	2.70	0.21	83
10	2.62	-0.23	2.70	0.14	79

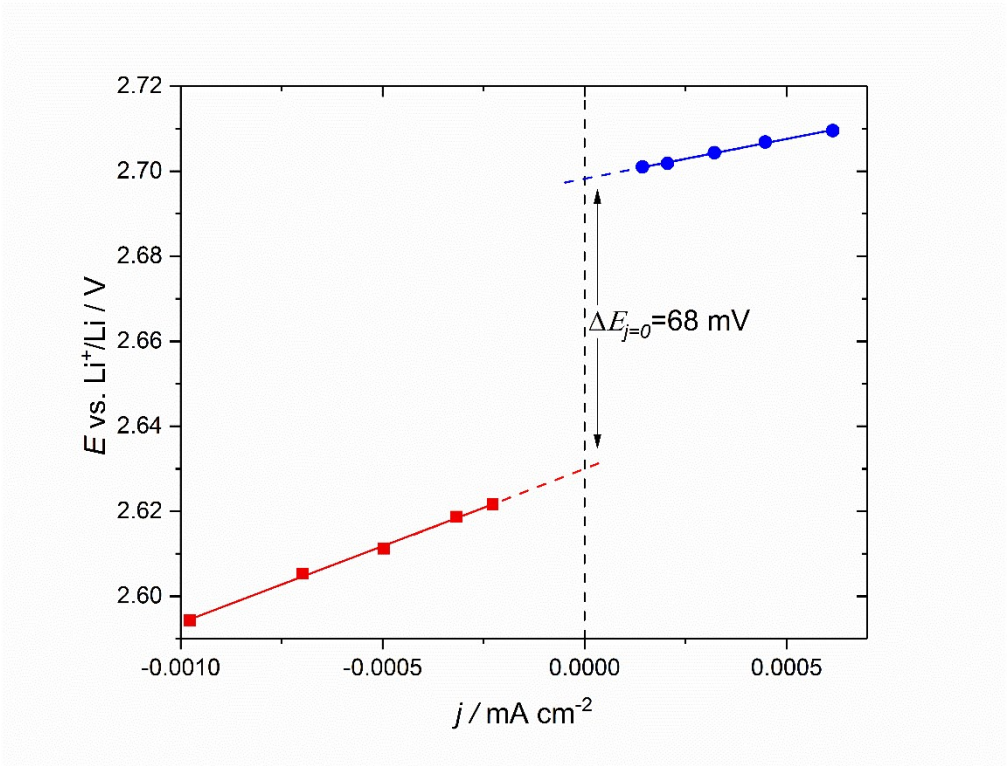

Figure S3: Peak potentials (E_{pc} and E_{pa}) plotted versus the peak currents (I_{pc} and I_{pa}), as obtained from the results in figure S2. A linear trend lines have been plotted to determine the peak-to-peak separation at zero current ($\Delta E_{j=0}$). Cathodic intercept = 2.630 V and anodic intercept = 2.698 V vs. Li^+/Li

Electrolysis measurements in a thin layer cell (figure S4) were performed to estimate the number of electrons involved in the first reduction process of $TBA_4SiW_{12}O_{40}$. A Swagelok cell was constructed with a $Li_{0.5}FePO_4$ counter electrode, a glass-fibre separator (Whatman®, glass microfiber filter, grade GF/F, Ø = 25 mm) wetted with 250 µl of 1 M LiTFSI DMSO electrolyte, lithium ion conducting glass ceramic (LICGC™, Ohara Corporation, Ø = 1 inch), a glass-fibre separator (Whatman®, glass microfiber filter, grade GF/F Ø = 15 mm) wetted with 125 µl of 5 mM $TBA_4SiW_{12}O_{40}$ in 1 M LiTFSI DMSO electrolyte and a carbon cloth working electrode (QuinTech, W0S1002P, Ø = 15 mm). A current collector with a greased inset O-ring (Polymax, Kalrez BS019) was pressed on to the stack which sealed against the Ohara glass. This ensured that the 125 µl of 5 mM $TBA_4SiW_{12}O_{40}$ in 1 M LiTFSI DMSO electrolyte in the working electrode compartment was completely sealed from the reference electrode electrolyte compartment. A potential step was applied from the open circuit potential (ca. 3 V vs. Li^+/Li) to 2.55 V vs. Li^+/Li and the current was measured (figure S4). Integration of the current with time gives a charge corresponding to 1.12 electrons per $TBA_4SiW_{12}O_{40}$, which indicates that the first reduction process corresponds to a one electron process.

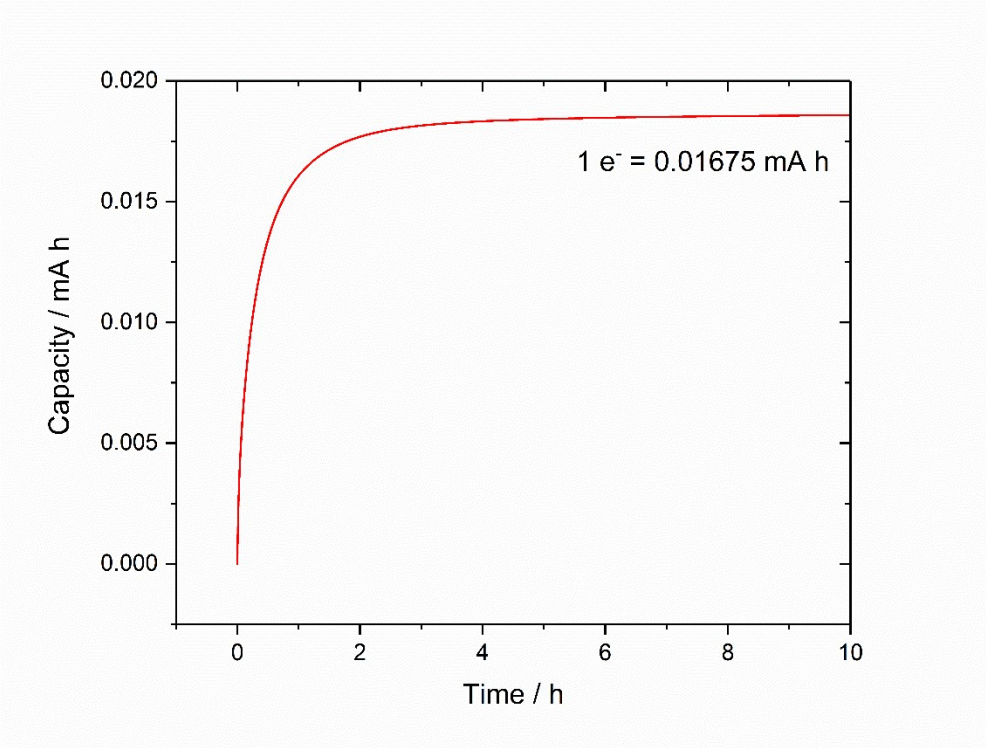

Figure S4: Chronoamperometry of carbon cloth working electrode in a Swagelok cell containing 125 µL of 5 mM $TBA_4SiW_{12}O_{40}$ in 1 M LiTFSI DMSO upon application of a potential step from the open circuit potential to 2.55 V vs. Li^+/Li.

Additional cyclic voltammetry measurements were performed with a glassy carbon electrode in the electrolyte 1 M LiTFSI DMSO without redox mediator with a low potential limit of 2.0 V vs. Li^+/Li (figure S5). The results show a marked decrease of the oxygen reduction current as the potential is scanned below ca. 2.55 V vs. Li^+/Li, which can be attributed to the passivation of the electrode surface by deposition of the discharge product Li_2O_2. The oxidation of Li_2O_2 to oxygen takes place at potentials higher than 3 V vs. Li^+/Li. In figure S6, the voltammograms recorded with a potential limit of 2.5 V vs. Li^+/Li are shown. By reversing the potential sweep at this higher potential, an oxidation wave is observed at potentials higher than around 2.7 V vs. Li^+/Li, which can be attributed to the oxidation of superoxide species formed during the oxygen reduction reaction, and at potentials higher than ca. 3 V vs. Li^+/Li a second broad oxidation peak is observed with can be attributed to the oxidation of Li_2O_2.

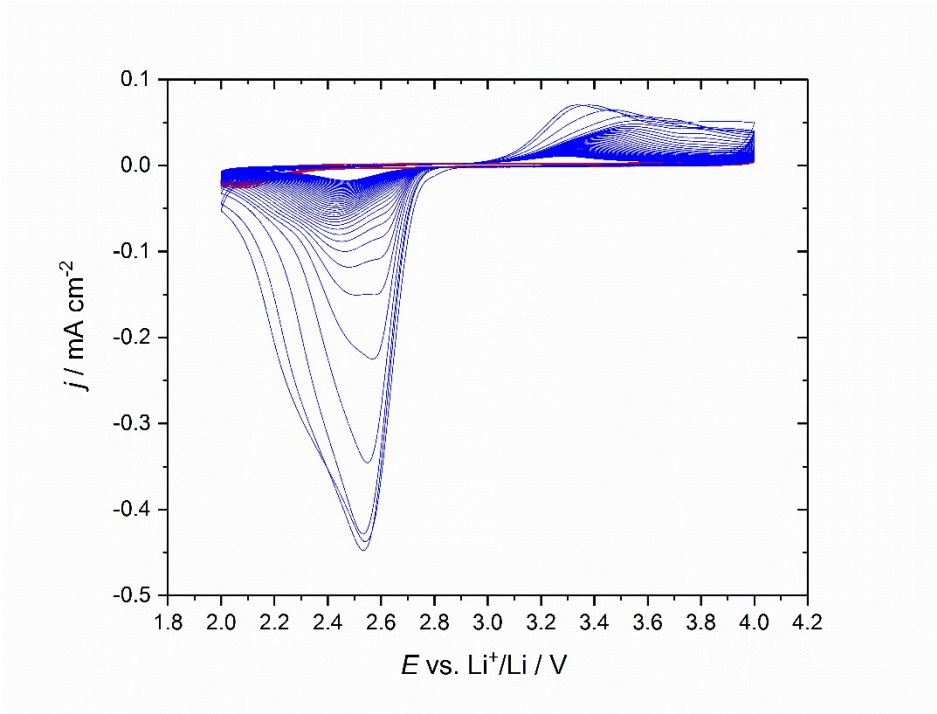

Figure S5: Cyclic voltammograms of a glassy carbon electrode an argon-saturated (red) and oxygen-saturated (blue) solutions of 1 M LiTFSI in DMSO, recorded at a scan rate of 20 mV s^{-1}, swept negative from the open circuit potential. A decrease in the magnitude of the current with cycle number is observed.

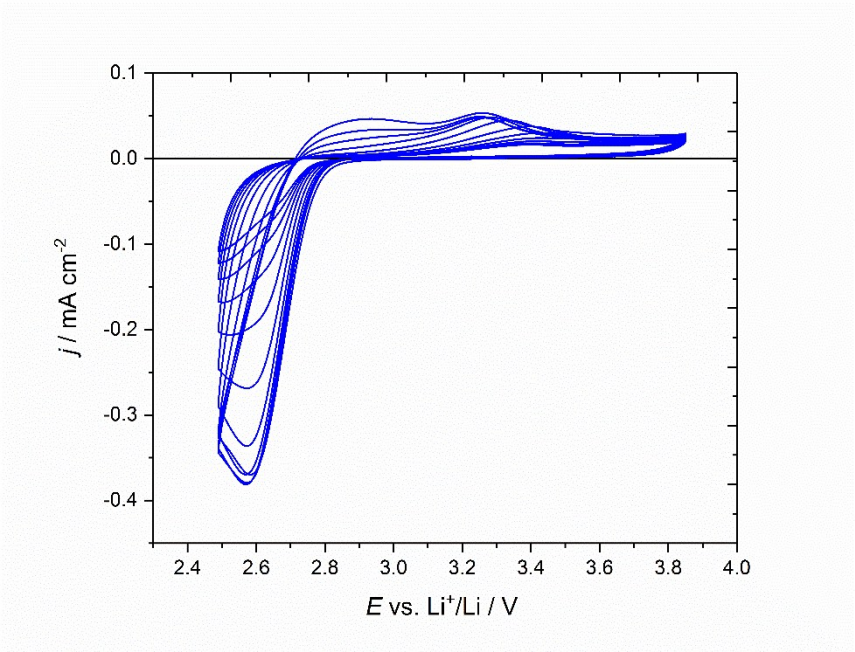

Figure S6: As seen in figure S5, but using a potential limit of 2.5 V vs. Li^+/Li. These results are the blue curves shown in figure 1 of the main article.

Additional cyclic voltammogram measurements were done in oxygen-saturated solutions with 10 mM $TBA_4SiW_{12}O_{40}$ in 1 M LiTFSI in DMSO (figure S7). As discussed in the main article, the decrease in the magnitude of the current with cycle number is significantly smaller than in the absence of redox mediator (figure S6).

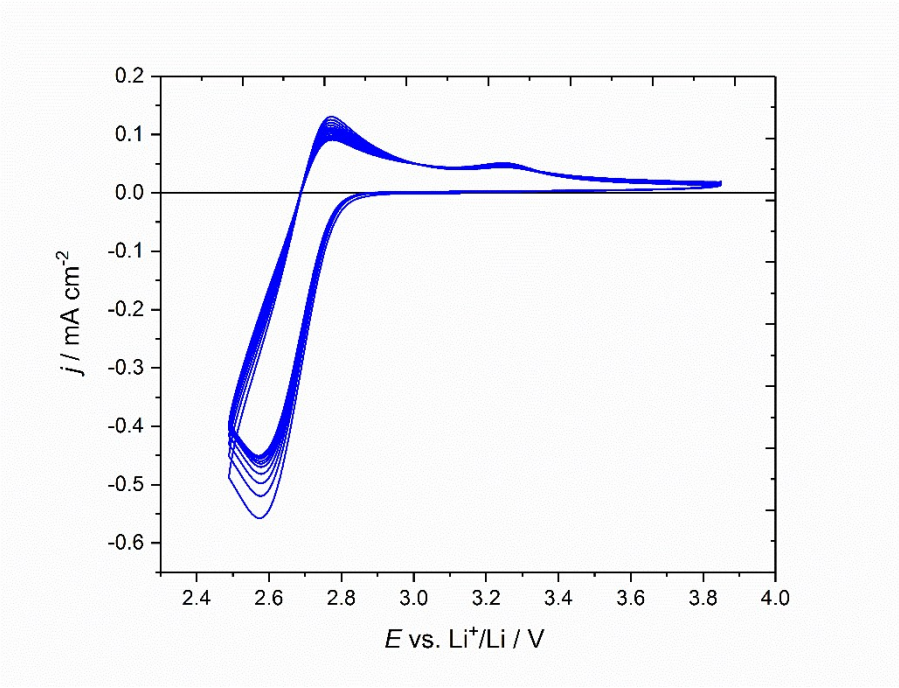

Figure S7: As figure S5, but using an oxygen-saturated solution with 10 mM $TBA_4SiW_{12}O_{40}$ in 1 M LiTFSI in DMSO and a potential limit of 2.5 V vs. Li^+/Li. These results are the red curves shown in figure 1 of the main article.

Galvanostatic cycling was performed in Swagelok cells containing a home-made current collector that allowed the supply of oxygen to the working electrode compartment (as detailed above). Figures S8 and S9 shows the results obtained upon application of different currents using a carbon cloth working electrode. Capacities have been normalized to the geometrical area of the carbon cloth electrode (3.14 cm^2), since the carbon cloth electrode is relatively thick (200 μm) and hence most of the carbon material remains inactive in these experiments, and therefore, the normalization by the mass of carbon (ca. 31 mg) is less appropriate. Figure S10 shows the discharge profile obtained using a Celgard separator coated with acetylene black carbon as the working electrode (see details in the experimental section above). It is well known that experimental discharge capacities in Li-O_2 cells markedly depend on experimental parameters such as electrode thickness and structure. Therefore, our results of the improvement of the capacity upon addition of the redox mediator (as evaluated by the ratio of discharge capacities with and without redox mediators) are compared with some previous work in table 2. The improvement observed upon addition of $TBA_4SiW_{12}O_{40}$ is comparable to other redox mediators in the literature, while the chemical and structural stability of $TBA_4SiW_{12}O_{40}$ could be superior.

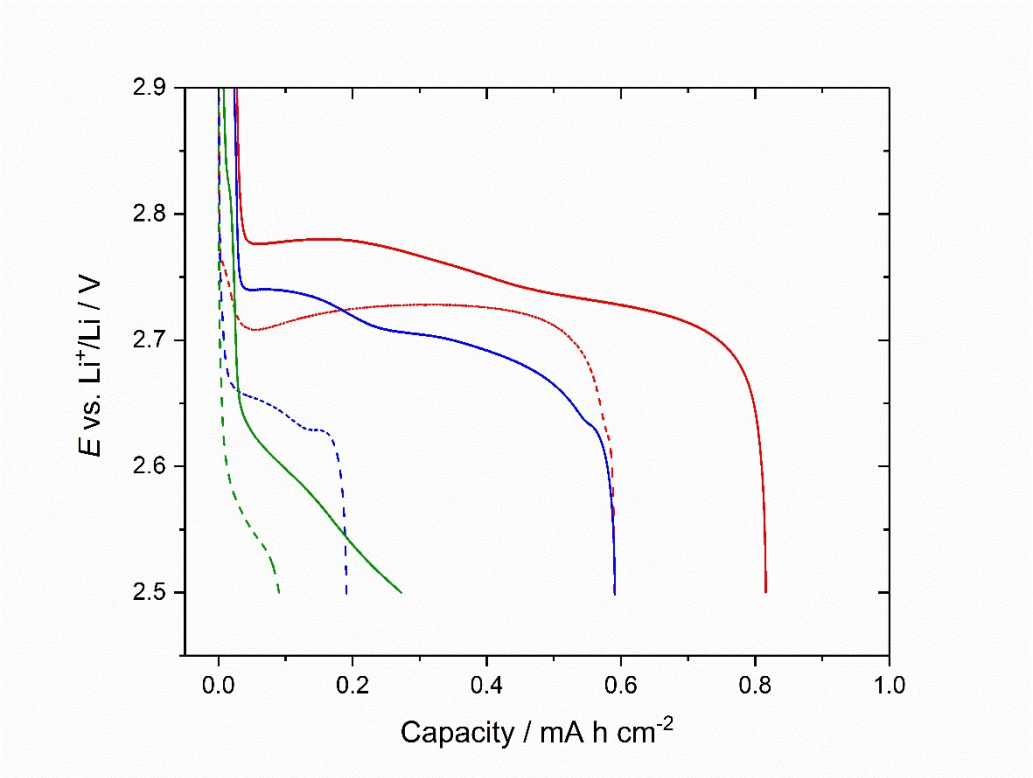

Figure S8. Galvanostatic discharge of Li-O_2 cells with (solid line) and without (dashed line) 50 mM $TBA_4SiW_{12}O_{40}$ in 1 M LiTFSI in DMSO at 15.9 μA cm^{-2} (red), 31.8 μA cm^{-2} (blue) and 63.7 μA cm^{-2} (green). The cells contain an Ohara glass membrane to separate the lithium electrode compartment, which contains no $TBA_4SiW_{12}O_{40}$. A carbon cloth (area: 3.14 cm^2) is used as the working electrode.

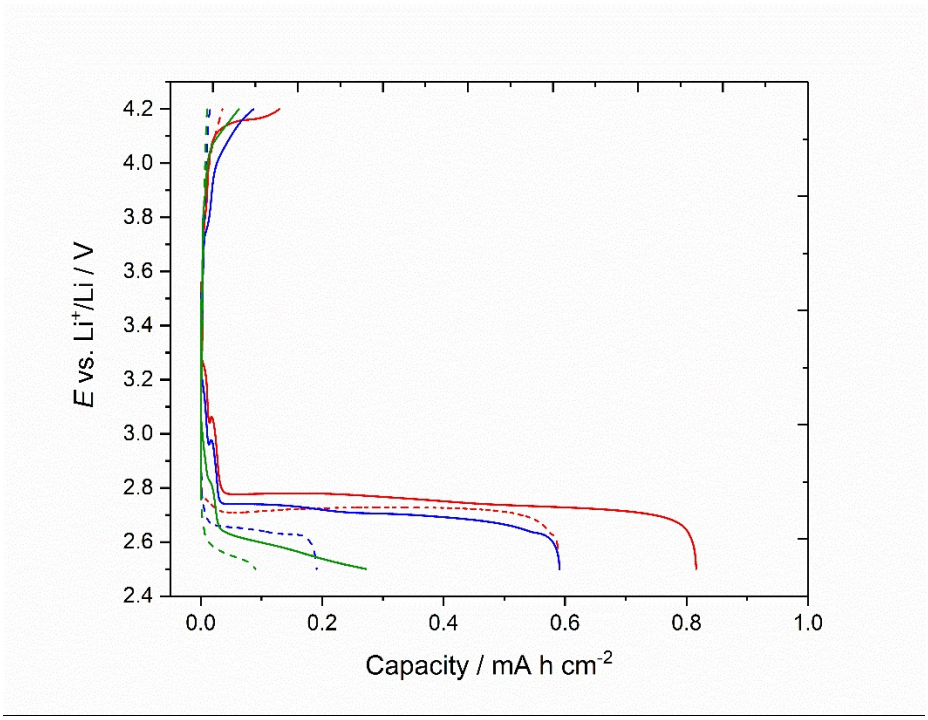

Figure S9. As in figure S8, but showing the re-charge of the cells as well as the discharge.

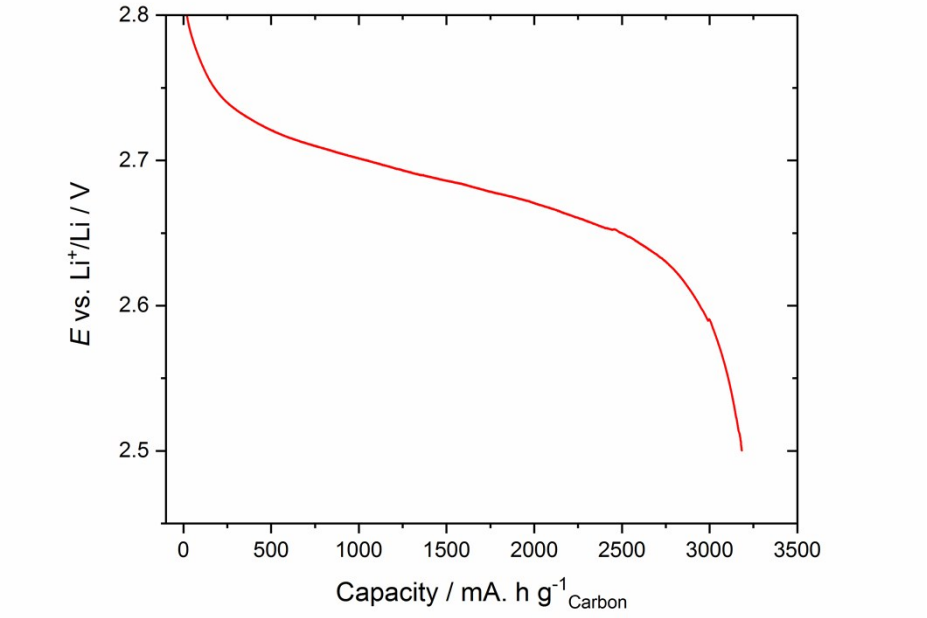

Figure S10. As in figure S8, but using a carbon-coated Celgard working electrode (area: 1.33 cm^2, carbon content ca 0.35 mg cm^{-2}) with 50 mM $TBA_4SiW_{12}O_{40}$ in 1 M LiTFSI in DMSO at 15 µA cm^{-2} (50 mA g^{-1}).

Table S2: Comparison of the improvement in discharge capacity with addition of mediators or other additives

Discharge mediator	**Discharge capacity without mediator (discharge rate in brackets)** C_1	**Discharge capacity with mediator (discharge rate in brackets)** C_2	**Capacity enhancement factor** C2/C1
Iron phthalocyanine (FePC)[3]	~2.0 mA h cm^{-2} (0.5 mA cm^{-2})	~3.2 mA h cm^{-2} (0.5 mA cm^{-2})	1.6
Ethyl viologen ($EtV(OTf)_2$)[4]	~ 2.0 µA h cm^{-2} (0.02 mA cm^{-2})	~ 4.8 µA h cm^{-2} (0.02 mA cm^{-2})	2.4
2,5-di-tert-butyl-1,4-benzoquinone (DBBQ)[5]	~ 0.13 mA h cm^{-2} (0.2 mA cm^{-2})	10.6 mA h cm^{-2} (0.2 mA cm^{-2})	~80
tris(2,4,6-trichlorophenyl)methyl (TTM) radical[6]	~3.5 mA h cm^{-2} (0.1 mA cm^{-2})	~7.5 mA h cm^{-2} (0.1 mA cm^{-2})	2.1
2,6-di-tert-butyl-hydroxytoluene (BHT)[7]	1.6 mA h cm^{-2} (0.1 mA cm^{-2})	2.7 mA h cm^{-2} (0.1 mA cm^{-2})	1.7
Phenol[8]	0.26 mA h cm^{-2} (0.05 mA cm^{-2})	9.1 mA h cm^{-2} (0.05 mA cm^{-2})	35
Coenzyme Q_{10} (CoQ_{10})[9]	15.7 mA h cm^{-2} (0.1 mA cm^{-2})	570 mA h cm^{-2} (0.1 mA cm^{-2})	36
$TBA_4SiW_{12}O_{40}$ (present work)	0.2 mA h cm^{-2} (0.03 mA cm^{-2})	0.6 mA h cm^{-2} (0.03 mA cm^{-2})	3

Additional characterisation of $TBA_4SiW_{12}O_{40}$

FT-IR measurements of the as prepared $TBA_4SiW_{12}O_{40,}$ after purification and drying, were acquired using a Nicolet iS5 FTIR Spectrometer (figure S11). The corresponding spectra of $TBA_4SiW_{12}O_{40}$ was compared to previous data published by Rocchiccioli-Deltcheff et al.[1] There was reasonable agreement between the two results. In addition, no broad peak is visible between the region 3100-3700 cm^{-1}; typically a water H_2O stretch, which shows that water content of the $TBA_4SiW_{12}O_{40}$ powder after drying was negligible.

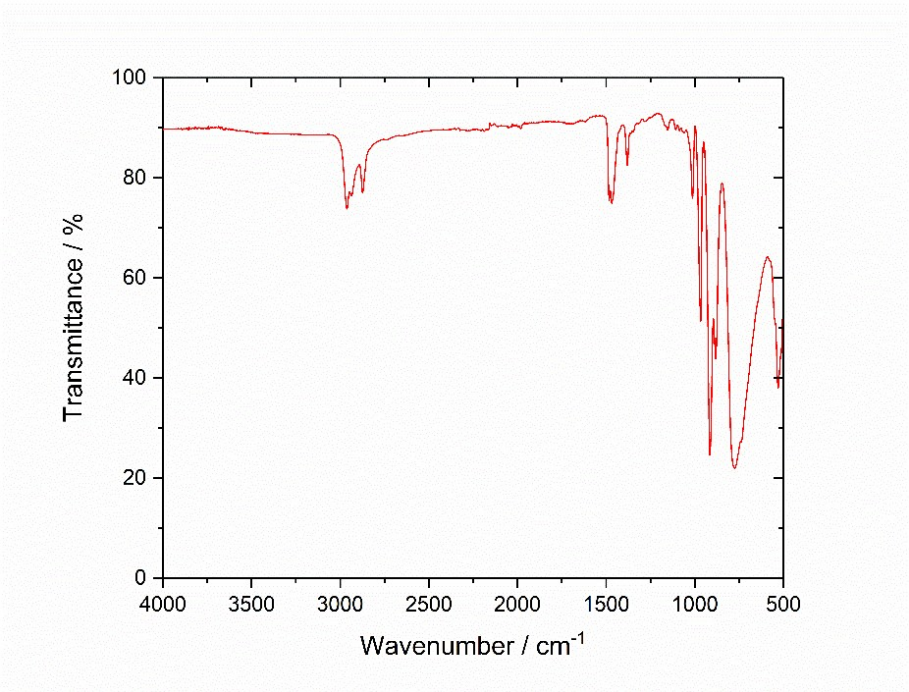

Figure S11: FT-IR spectrum of the as prepared $TBA_4SiW_{12}O_{40}$, after purification and drying.

Table S3: Comparison of the FTIR characteristic bands of the $TBA_4SiW_{12}O_{40}$ prepared in this study with the previously published data by Rocchiccioli-Deltcheff et al.[1]
Vs- very strong, s –strong, m-medium, w-weak, vw-very weak, sh-shoulder

C.Rocchiccioli-Deltcheff data[1]	Experimental data
1011 (m)	1013 (w)
967 (s)	966 (s)
920 (vs)	915 (vs)
883 (m)	882 (m)
797 (vs)	776 (vs)
542 (m)	530 (m)

Raman measurements of the as prepared $TBA_4SiW_{12}O_{40,}$ after purification and drying, were acquired using a Renishaw InVia microscope equipped with a 785 nm He-Ne laser (figure S12). $TBA_4SiW_{12}O_{40}$ spectra were acquired using 100 mV power (at 1% power) with a single acquisition time of 10s and a 50X objective. The spectra and corresponding peaks were compared with previously published data[1]. The peaks had no omissions and displayed good accord with previous findings.

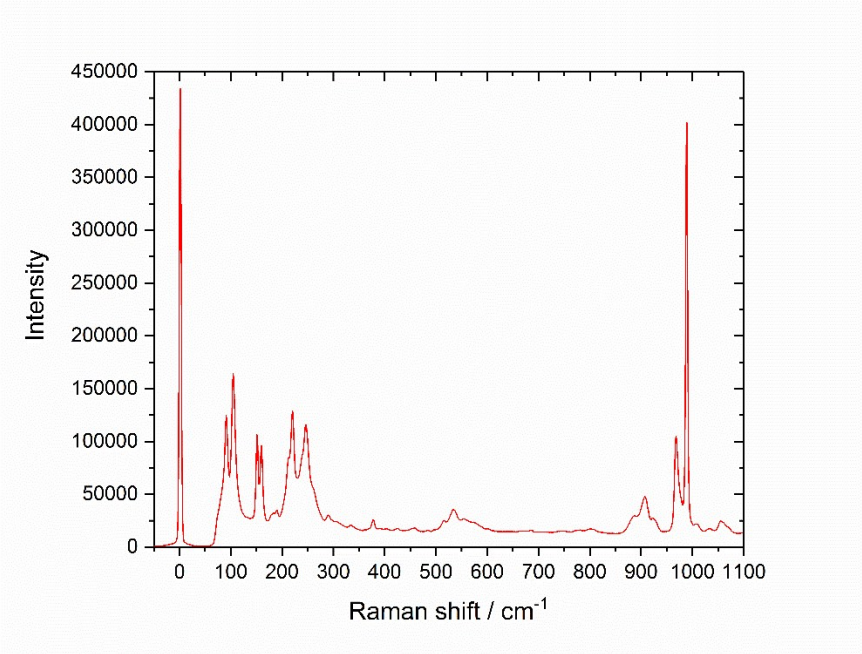

Figure S12: Raman spectrum of the as prepared $TBA_4SiW_{12}O_{40}$, after purification and drying.

Table S4: Comparison of the Raman characteristic bands of the $TBA_4SiW_{12}O_{40}$ prepared in this study with the previously published data by Rocchiccioli-Deltcheff et al.[1]
Vs- very strong, s –strong, m-medium, w-weak, vw-very weak, sh-shoulder

C.Rocchiccioli-Deltcheff et al.[1]	Experimental data	C.Rocchiccioli-Deltcheff et al.[1]	Experimental data
1009 (w)	1010 (w)	288 (w)	290 (w)
987 (vs)	989 (vs)	244.5 (m)	246 (m)
966 (s)	968 (s)	218.5 (s)	220 (s)
924 (w)	923 (w)	210.5 (sh)	212 (sh)
906 (m)	908 (m)	187 (w)	189 (w)
886 (w)	886 (w)	157.5 (s)	160 (s)
560 (sh)	558 (sh)	149.5 (s)	151 (s)
533 (m)	534 (m)	102.5 (s)	104 (s)
376 (w)	378 (w)	89 (s)	91 (s)

UV–vis measurements were carried out using a Perkin Elmer Lambda XLS UV-vis spectrometer (figure S13). Quartz cuvettes with screw caps (Starna, path length = 1 cm) were used. A solution of 15 mM $TBA_4SiW_{12}O_{40}$ in DMSO was prepared and diluted to 0.015 mM by serial dilution, and UV-vis measurements were performed using pure DMSO as reference. An absorbance band at 260 nm shares good agreement with previous literature.[10,11]

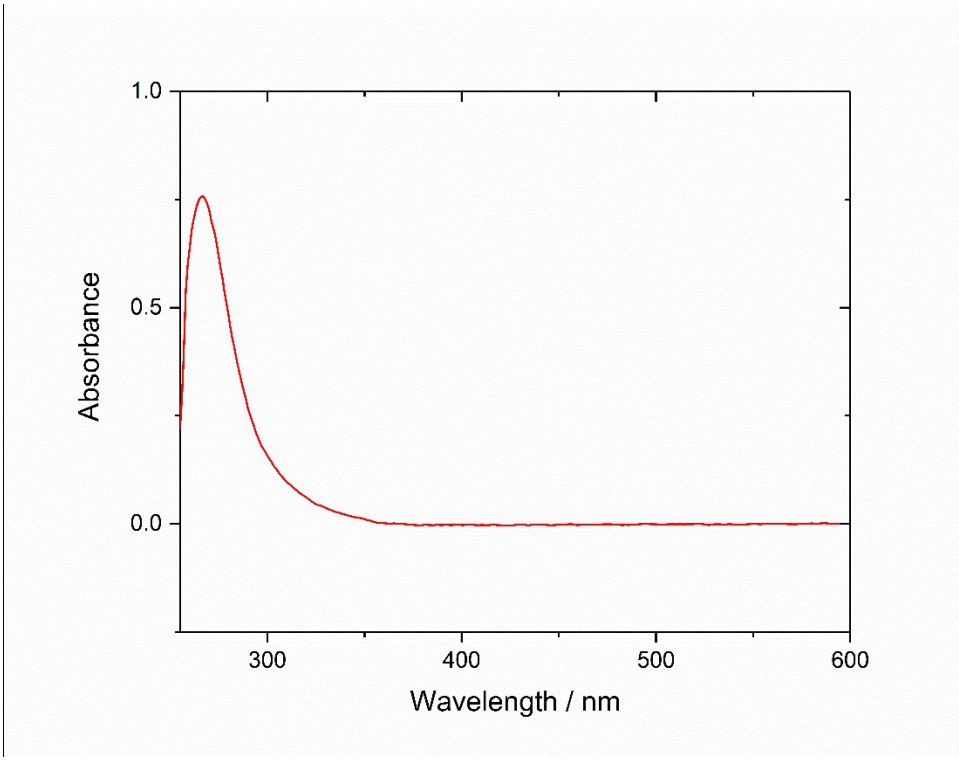

Figure S13: UV-vis spectrum of a solution of 0.015 mM $TBA_4SiW_{12}O_{40}$ in DMSO

Stability of $TBA_4SiW_{12}O_{40}$ in the presence of superoxide

The stability of solutions of $TBA_4SiW_{12}O_{40}$ in DMSO in the presence of KO_2 was characterized with UV–vis measurements. A solution of 6 mM KO_2 in DMSO was prepared and diluted to 0.6 mM by serial dilution, and the UV-vis measurements were taken, using pure DMSO as reference (figure S14). Small variations in the band intensity could be due to reaction of KO_2 with impurities (e.g. water traces). Then, a solution containing 0.6 mM KO_2 and 0.015 mM $TBA_4SiW_{12}O_{40}$ in DMSO was prepared by mixing equal volumes of solutions of 1.2 mM KO_2 and 0.03 mM $TBA_4SiW_{12}O_{40}$ in DMSO, which were prepared by serial dilution from more concentrated solutions of 6 mM KO_2 and 15 mM $TBA_4SiW_{12}O_{40}$ in DMSO, respectively. The UV-vis measurements of the mixed solution containing $TBA_4SiW_{12}O_{40}$ and KO_2, using pure DMSO as reference, are shown in figure S15. The variation of the band intensity over time is small, suggesting that no reaction of $TBA_4SiW_{12}O_{40}$ and KO_2 takes place, that is, $TBA_4SiW_{12}O_{40}$ is stable in the presence of KO_2 in DMSO.

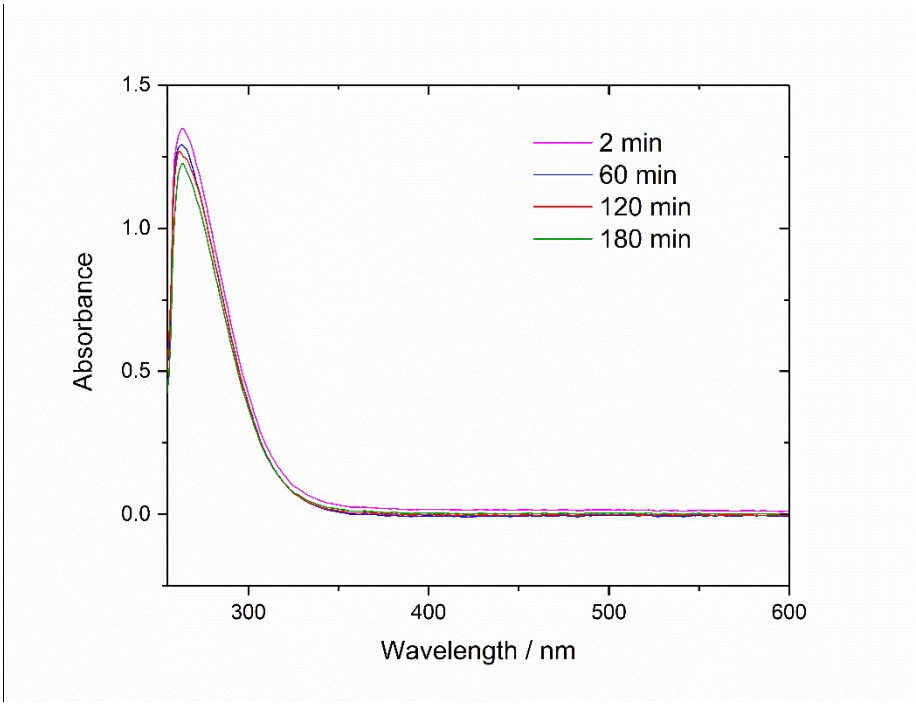

Figure S14: UV-vis spectrum of a solution of 0.6 mM KO_2 in DMSO over time.

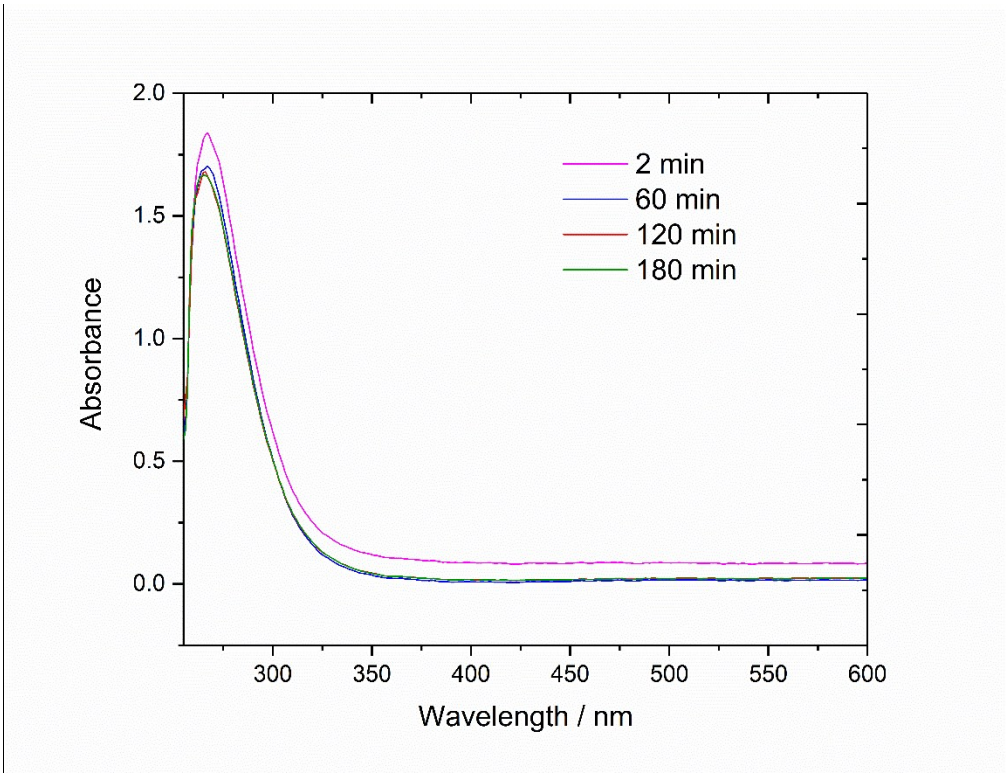

Figure S15: UV-vis spectrum of a solution of 0.015 mM $TBA_4SiW_{12}O_{40}$ + 0.6 mM KO_2 in DMSO over time.

Characterization of the discharged electrode with SEM

SEM measurements were performed on a discharged carbon-coated electrode using a JSM 6500 scanning electron microscope.

A Swagelok cell containing a carbon-coated Celgard cathode (Ø = 25 mm) with 50 mM $TBA_4SiW_{12}O_{40}$ in 1 M LiTFSI DMSO was purged with O_2 and subject to a discharge current of 4 µA cm^{-2} for 96 hours. Immediately after discharge, the cell was transferred to an argon-filled glove box and the cathode was removed from the cell and transferred onto an aluminium stub with an affixed conductive carbon tape for SEM measurements.

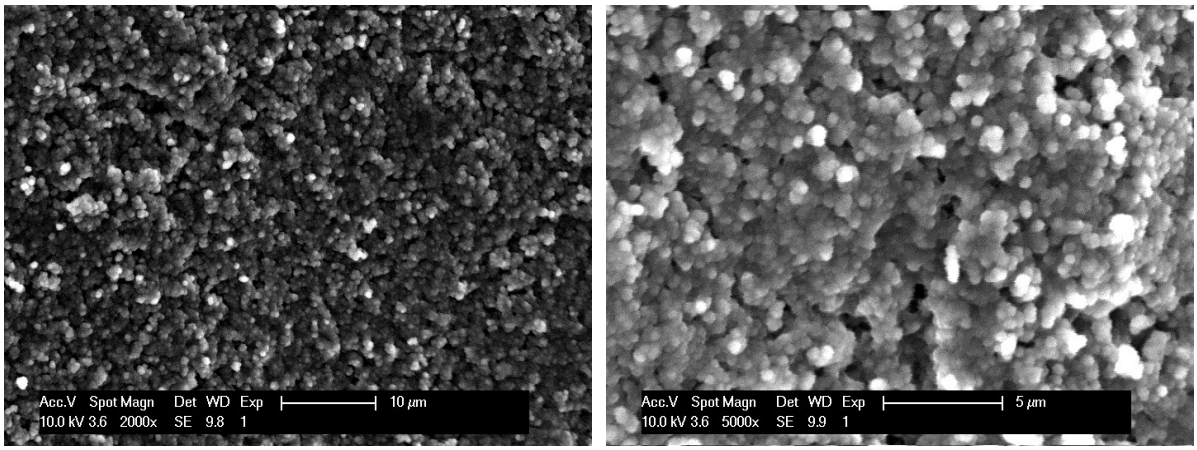

Figure S16: SEM images of a carbon-coated electrode discharged at 20 µA in 50 mM $TBA_4SiW_{12}O_{40}$ in 1 M LiTFSI DMSO.

References

1 C. Rocchiccioli-Deltcheff, M. Fournier, R. Franck and R. Thouvenot, *Inorg. Chem.*, 1983, **22**, 207–216.

2 N. Intaranont, N. Garcia-Araez, A. L. Hector, J. A. Milton and J. R. Owen, *J. Mater. Chem. A*, 2014, **2**, 6374–6377.

3 D. Sun, Y. Shen, W. Zhang, L. Yu, Z. Yi, W. Yin, D. Wang, Y. Huang, J. Wang, D. Wang and J. B. Goodenough, *J. Am. Chem. Soc.*, 2014, **136**, 8941–8946.

4 L. Yang, J. T. Frith, N. Garcia-Araez and J. R. Owen, *Chem. Commun.*, 2015, **51**, 1705–1708.

5 X. Gao, Y. Chen, L. Johnson and P. G. Bruce, *Nat. Mater.*, 2016, **15**, 882–888.

6 A. Y. Tesio, D. Blasi, M. Olivares-Marín, I. Ratera, D. Tonti and J. Veciana, *Chem. Commun.*, 2015, **51**, 17623–17626.

7 W. Yu, W. Yang, R. Liu, L. Qin, Y. Lei, L. Liu, D. Zhai, B. Li and F. Kang, *Electrochem. commun.*, 2017, **79**, 68–72.

8 X. Gao, Z. P. Jovanov, Y. Chen, L. R. Johnson and P. G. Bruce, *Angew. Chemie - Int. Ed.*, 2017, **56**, 6539–6543.

9 Y. Zhang, L. Wang, X. Zhang, L. Guo, Y. Wang and Z. Peng, *Adv. Mater.*, 2018, **30**.

10 G. M. Varga, E. Papaconstantinou and M. T. Pope, *Inorg. Chem.*, 1970, **9**, 662–667.

11 P. Gómez-Romero and N. Casañ-Pastor, *J. Phys. Chem.*, 1996, **100**, 12448–12454.